StrucOpt manuscript No.
(will be inserted by the editor)

Detecting stress fields in an optimal structure I Two-dimensional case and analyzer

A. Cherkaev and İ. Küçük

Abstract In this paper, we investigate the stress field in optimal elastic structures by the necessary conditions of optimality, studying two-phase elastic composites in two dimensions. Necessary conditions show that an optimal design is characterized by three zones: *Zone 1* of pure weak *Material 1*; *Zone 2* of pure strong *Material 2*; *Zone 3* where *Material 1* and *Material 2* are mixed to form an optimal microstructure. To characterize these zones we introduce two rotationally invariant norms $\mathcal{N}_1$ and $\mathcal{N}_2$ of a stress tensor. The derived optimality conditions state that inequality $\mathcal{N}_1(\boldsymbol{\sigma}) < constant_1$ holds in *Zone 1*; inequality $\mathcal{N}_2(\boldsymbol{\sigma}) > constant_2$ holds in *Zone 2*; and two equalities hold simultaneously in *Zone 3*: $\mathcal{N}_1(\boldsymbol{\sigma}) = constant_1$, in the *Material 1*; $\mathcal{N}_2(\boldsymbol{\sigma}) = constant_2$ in the *Material 2*. Using this result, we analyze suboptimal projects and find how close fields there are to the regions of optimality.

1 Introduction

Structural optimization asks for the "best" layout of two elastic materials in a design domain. Problems of this kind are examples of *nonconvex multivariable variational problems*; they require minimization of an integral if a non-convex Lagrangian that depends on fields, such as the stress fields in elasticity. More specifically, the Lagrangian of the considered problem is a two-well function: A minimum of two convex functions (wells) that correspond to the energies of each phase.

The nonconvexity of the Lagrangian yields to nonexistence of a classical (variational) solution, to the necessity to build special highly oscillating minimizing sequences and develop special methods for relaxation of the Lagrangian. The most popular method to handle the unstable problem is similar to the Ritz method: A class of special oscillating minimizing sequences called laminated of a rank, that is laminates made of laminates, is considered. The averaged properties of these structures can be analytically calculated. They depend on several geometric parameters which are adjusted to improve the solution. Another method (translation method) is based on sufficient conditions of optimality: a lower bound of the nonconvex Lagrangian is build that leads to a smooth solution of the *relaxed* variational problem. This new solution is in fact the average stress field in an optimal structure. To build the bound, the differential properties of the solution (like the divergence-free character of stresses) are replaced by a weaker requirements.

Both methods were applied to several problems of structural optimization, including to the problem under study. They provide the complete picture of the solution when the minimum achieved on minimizing sequences matches the lower bound. However, both methods have serious limitations: The "laminates" method critically depends on the correctness of a priori guess about the class of proper structures, and the translation method can lead to violation of the differential properties of solution and to a slack bound. Therefore, a more universal method is needed to investigate the structural optimization problems that is free of strong a priori guesses. Looking for such method, we turn to a classical variational technique of strong local variations, developed in Lurie (1975) and applied to the structural optimization in early papers: Lurie (1975) and Lurie and Cherkaev (1978) . Last years, this technique was further developed in the book Cherkaev (2000) where conducting designs were considered. The technique we used in this paper can be generalized to sum of the energies for multiple loading case Cherkaev et al. (1998b).

In this paper, we develop the method of necessary conditions and apply it to elastic structures. The stress field in optimal elastic structures is investigated by means of special conditions of optimality. We consider the well investigated problem of the optimal layout of two-phase elastic composites in two dimensions. This allows us to compare the suggested method with the known ones. The discussed problem has already been studied from

Received: August 28, 2001

A. Cherkaev and İ. Küçük

Department of Mathematics, University of Utah, Salt Lake City, 84108, USA
e-mail: `cherk@math.utah.edu` and e-mail: `kucuk@math.utah.edu`

various perspectives (see recent review, Eschenauer and Olhoff (2001)): The lower bound of the energy among all structures was calculated by means of the *translation method*, see Gibiansky and Cherkaev (1997); Allaire and Kohn (1994); Grabovsky (1996a). It was shown that the optimal structures are either second-rank laminates Gibiansky and Cherkaev (1997); Milton (1981) or, in some special cases, *Vigdergauz structures* Vigdergauz (1989); Grabovsky and Kohn (1995) or *Hashin's coated spheres* Hashin and Shtrikman (1962).

It is possible that other microstructures exist that are optimal as well, which brings up the question: What do these structures have in common? Our analysis of optimal fields answers this question. The necessary conditions approach supplement the mentioned results by analysis of the fields in an optimal structure without a priori specification of admissible geometric configurations. We are not checking the properties of guessed geometries, but describing the fields in all optimal structures.

In this paper, we derive the optimality conditions and characterize the stress fields in both materials mixed in the optimal design. We also analyze suboptimal projects to judge how close they are to the optimum. Finally, we compare the necessary conditions of optimality with sufficient conditions. The discussed technique can also be applied to more general problems: The minimization the energy of multi-material mixtures (see Cherkaev (2000)) or the minimization of other functionals.

2 Formulation of the problem

Consider a domain Ω that is divided into two subdomains $\Omega_i,\ i=1,2$. The subdomains Ω_i are occupied by isotropic materials with bulk and shear moduli of κ_i and μ_i, respectively. Suppose that the volumes of Ω_1 and Ω_2 are fixed and a load is applied from the boundary.

A linearly elastic structure at equilibrium and in the absence of body forces satisfies the following elasticity equations (see, for example, Timoshenko (1970), Fung (1965), and Atkin and Fox (1980))

$$\nabla\cdot\boldsymbol{\sigma}(x)=0, \qquad \boldsymbol{\epsilon}=\frac{1}{2}(\nabla u+(\nabla u)^T), \qquad \boldsymbol{\epsilon}(x)=\boldsymbol{\mathcal{S}}(x)\boldsymbol{\sigma}(x), \tag{1}$$

where u is a deflection vector, $\boldsymbol{\sigma}(x)$, and $\boldsymbol{\epsilon}(x)$ are stress and strain fields respectively and $\boldsymbol{\mathcal{S}}(x)$ is the compliance tensor that characterizes the material properties.

The density of the energy is given by

$$\boldsymbol{\mathcal{G}}(\chi,\boldsymbol{\sigma})=\frac{1}{2}\boldsymbol{\sigma}(x):\boldsymbol{\mathcal{S}}(x):\boldsymbol{\sigma}(x), \tag{2}$$

where the second-rank stress tensors $\boldsymbol{\sigma}(x)$ belong to the set $\mathcal{F}^s(x)$ of statically admissible stress fields (see (1).)

$$\mathcal{F}^s(x)=\{\boldsymbol{\sigma}(x)\mid\nabla\cdot\boldsymbol{\sigma}(x)=0\ in\ \Omega,\boldsymbol{\sigma}(x)\mathbf{n}(x)=\mathbf{t}(x)\ on\ \Gamma_T\}. \tag{3}$$

Here, $\mathbf{t}(x)$ is surface traction, $\mathbf{n}(x)$ is the normal to the surface, and Γ_T is the boundary component where the traction is applied.

In (2), $\boldsymbol{\mathcal{S}}(x)$ is a fourth-rank material compliance tensor of the heterogeneous material. The set of compliance tensors, $\boldsymbol{\mathcal{S}}_{ad}$, consists of the tensors:

$$\boldsymbol{\mathcal{S}}(x)=\boldsymbol{\chi}(x)\boldsymbol{\mathcal{S}}_1(\mu_1,\kappa_1)+(1-\boldsymbol{\chi}(x))\boldsymbol{\mathcal{S}}_2(\mu_2,\kappa_2), \tag{4}$$

where μ_i and κ_i are shear and bulk moduli of each material, and $\chi(x)$ is the characteristic function:

$$\chi(x)=\begin{cases}0 & \text{if } x\in\Omega_1,\\ 1 & \text{if } x\in\Omega_2.\end{cases} \tag{5}$$

Using the principle of minimum total stress energy, we can reformulate the elasticity equation as the minimizer for the total energy $\mathsf{E}(\chi)$

$$\mathsf{E}(\chi)=\min_{\boldsymbol{\sigma}(x)\in\mathcal{F}^s(x)}\int_\Omega\boldsymbol{\mathcal{G}}(\chi,\boldsymbol{\sigma})d\Omega. \tag{6}$$

where the stress field $\boldsymbol{\sigma}(x)$ minimizes the total stress energy (or maximizes the total stiffness).

Consider now an optimization problem

$$\mathcal{J}=\min_{\chi(x)}\mathcal{W}(\chi);\quad \mathcal{W}(\chi)=[\mathsf{E}(\chi)+\gamma_1\chi+\gamma_2(1-\chi)], \tag{7}$$

where γ_1 and γ_2 are the cost of *Material 1* and *Material 2*, respectively. The optimization problem (7) leaves the possibility of fine-scale oscillations of the control $\chi(x)$ (see, for example, Cherkaev (2000)). Physically speaking, these oscillations require that the optimally designed structure is a *composite*. The composites properties represent limits of rapidly oscillating sequences of the original layout. To deal with the fast oscillating solutions to optimization problems, *relaxation* techniques are developed, see Cherkaev (2000). Relaxation essentially averages the solution of an optimization problem by replacing the heterogeneous medium with the composite with the optimal effective properties.

Matrix Representation for a Fourth Rank Plane Tensor Dealing with tensor calculations, it is convenient to transform tensors into matrices and vectors in a tensor space. Let us consider the following base:

$$\mathbf{b}^{(1)}=\tfrac{1}{\sqrt{2}}\begin{pmatrix}1&0\\0&-1\end{pmatrix},\qquad \mathbf{b}^{(2)}=\tfrac{1}{\sqrt{2}}\begin{pmatrix}0&1\\1&0\end{pmatrix},\qquad \mathbf{b}^{(3)}=\tfrac{1}{\sqrt{2}}\begin{pmatrix}1&0\\0&1\end{pmatrix}. \tag{8}$$

where $\mathbf{b}^{(i)} = \{b^{(i)}_{\alpha\beta}\}$. In this base, any symmetric forth-rank tensor can be rewritten as a three by three matrix while any symmetric second-rank tensor can be represented by a three-dimensional vector.

A second-rank stress tensor has the following representation,

$$\sigma_{\alpha\beta} = \sigma_{\kappa\eta} b^{(i)}_{\kappa\eta} b^{(i)}_{\alpha\beta} = \mathrm{s}_1 b^{(1)}_{\alpha\beta} + \mathrm{s}_2 b^{(2)}_{\alpha\beta} + \mathrm{s}_3 b^{(3)}_{\alpha\beta} \tag{9}$$

where $(\mathrm{s}_1\ \mathrm{s}_2\ \mathrm{s}_3)^T = \mathbf{s}$ is a vector with the components,

$$\mathrm{s}_1 = \frac{\sigma_{11} - \sigma_{22}}{\sqrt{2}}, \quad \mathrm{s}_2 = \frac{2}{\sqrt{2}}\sigma_{12} \ \ and \ \ \mathrm{s}_3 = \frac{\sigma_{11} + \sigma_{22}}{\sqrt{2}}, \tag{10}$$

and an anisotropic fourth-rank compliance tensor $\boldsymbol{\mathcal{S}}$ is replaced by a symmetric three by three matrix $\boldsymbol{\mathcal{D}} = (\mathcal{D}_{ij})$. Components of $\boldsymbol{\mathcal{D}}$ are determined by the following transformation,

$$\mathcal{D}_{ij} = b^{(i)}_{\alpha\beta} \boldsymbol{\mathcal{S}}_{\alpha\beta\kappa\eta} b^{(j)}_{\kappa\eta}, \quad i, j = 1, 2. \tag{11}$$

The components of $\boldsymbol{\mathcal{D}}$ can be written as follows

$$\begin{aligned} \mathcal{D}_{11} &= \frac{1}{2}(\mathcal{S}_{1111} + \mathcal{S}_{2222}) - \mathcal{S}_{1122}, \\ \mathcal{D}_{12} &= \mathcal{S}_{1112} - \mathcal{S}_{2221}, \quad \mathcal{D}_{13} = \frac{1}{2}(\mathcal{S}_{1111} + \mathcal{S}_{2222}), \\ \mathcal{D}_{22} &= \frac{1}{2}(\mathcal{S}_{1111} + \mathcal{S}_{2222}) + \mathcal{S}_{1122}, \\ \mathcal{D}_{12} &= \mathcal{S}_{1112} + \mathcal{S}_{2221}, \quad \mathcal{D}_{33} = 2\mathcal{S}_{1212}. \end{aligned} \tag{12}$$

Particularly, a fourth-rank isotropic compliance tensor $\boldsymbol{\mathcal{S}}$ is given by a diagonal matrix,

$$\boldsymbol{\mathcal{D}}_i = diag\left(\frac{1}{2\mu_i}, \frac{1}{2\mu_i}, \frac{1}{2\kappa_i}\right). \tag{13}$$

Remark 1 Although we used a new notation $\boldsymbol{\mathcal{D}}$ for a transformed compliance tensor, the tensor notation $\boldsymbol{\mathcal{S}}$ will also be used for transformed compliance tensors hereafter.

3 Variations

3.1 The Scheme of the Weierstrass Test

We investigate the optimality of a design by means of necessary conditions of optimality, namely, the Weierstrass-type test. The Weierstrass-type *structural variation* is described next.

An array of infinitesimal inclusions of an admissible material $\boldsymbol{\mathcal{S}}_n$ is implanted at a point x in the domain Ω occupied by a host material $\boldsymbol{\mathcal{S}}_h$ (see Figure 1). We compare the cost of the problem with and without the implant, and compute the increment of the cost: The difference between the functional corresponding to the design with and without implant. If the examined structure is optimal, the increment is nonnegative. Otherwise, the cost is reduced by the variation, and the design fails the Weierstrass-type test.

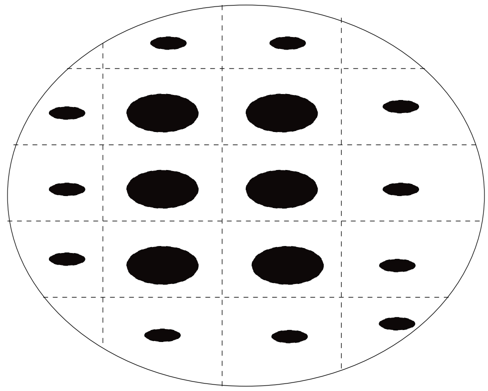

Fig. 1 A cartoon for inclusions in a base material. The volume fractions of inclusions is infinitely small.

The increment of energy depends on the shape of the region of variation and must stay positive no matter what this shape is. Accordingly, the shape must be adjusted to the field to minimize the increment that must remain nonnegative, see Lurie (1975).

3.2 Variation of Properties

The usual way to perform the Weierstrass-type variation is to consider an elliptical inclusion and to adjust it, see Lurie (1975). However, we use a slightly different procedure here. Namely, we consider the structural variation that is a dilute array (second-rank laminates) of elongated inclusions following Cherkaev (2000). In this structure, the inclusions are made of the (nuclei) material $\boldsymbol{\mathcal{S}}_n$, and the envelope is made of the host material $\boldsymbol{\mathcal{S}}_h$. This array is implanted into the pure host medium $\boldsymbol{\mathcal{S}}_h$.

First, we describe properties of a second-rank laminate. This composite structure can be characterized by its effective tensor $\boldsymbol{\mathcal{S}}_*$; the effective tensor that links the averaged stress and strain fields in the "representative region." This region is much larger than an individual inclusion, but much smaller than the region of variation. The effective tensor $\boldsymbol{\mathcal{S}}_*(m_n)$ of the structure depends on geometrical parameters of the inclusion array; its derivation uses the continuity conditions on the boundaries of the inclusions, see Cherkaev (2000). In our notations, it has the form:

$$\boldsymbol{\mathcal{S}}_*(m_n) = \boldsymbol{\mathcal{S}}_h + m_n \left((\boldsymbol{\mathcal{S}}_n - \boldsymbol{\mathcal{S}}_h)^{-1} + (1-m_n)\boldsymbol{\Delta}(\alpha) \right)^{-1}, \quad (14)$$

where m_n is the volume fraction of the nuclei and matrix $\boldsymbol{\Delta}$ depends on the structure of the array. In the base (8), where the coordinate axes coincide with the directions of lamination, matrix $\boldsymbol{\Delta}(\alpha)$ is

$$\boldsymbol{\Delta}(\alpha) = \frac{\kappa_h \mu_h}{\kappa_h + \mu_h} \begin{pmatrix} 1 & 0 & 2\alpha - 1 \\ 0 & 0 & 0 \\ 2\alpha - 1 & 0 & 1 \end{pmatrix}, \quad 0 \le \alpha \le 1. \quad (15)$$

Here, the inner parameter α is the relative elongation of inclusions in the array; this parameter is responsible for anisotropy of effective tensor $\boldsymbol{\mathcal{S}}_*$.

Remark 2 For the considered problem, the effective tensor $\boldsymbol{\mathcal{S}}_*(m_n)$ was calculated in the papers Gibiansky and Cherkaev (1997); Francfort and Murat (1986); Milton (1986); Bendsøe et al. (1993). In order to compute it, a two-step procedure is used: First, the effective property of a laminate made from initial materials is computed; then the effective property of a laminate made from the host material and the obtained laminate is computed by the same procedure. After proper simplifications, one arrives at the formula (14).

Suppose now that the volume fraction m_n is infinitesimal, $m_n = \delta m \ll 1$. The effective property $\boldsymbol{\mathcal{S}}_*(m + \delta m)$ can be calculated via Taylor's expansion:

$$\boldsymbol{\mathcal{S}}_*(m + \delta m) = \boldsymbol{\mathcal{S}}_*(m) + \delta m \frac{d}{dm} \boldsymbol{\mathcal{S}}_*(m) + \mathsf{o}(\delta m) \quad (16)$$

Substituting the value of $\boldsymbol{\mathcal{S}}_*(m)$ from (14) into (16), we obtain

$$\boldsymbol{\mathcal{S}}_*(\delta m) \cong \boldsymbol{\mathcal{S}}_h + \delta \boldsymbol{\mathcal{S}},$$

where

$$\delta \boldsymbol{\mathcal{S}} = \mathbf{V} \delta m + \mathsf{o}(\delta m), \quad \mathbf{V} = \left((\boldsymbol{\mathcal{S}}_n - \boldsymbol{\mathcal{S}}_h)^{-1} + \boldsymbol{\Delta} \right)^{-1}, \quad (17)$$

and $\boldsymbol{\Delta}$ is defined in (15).

Next, compute variation of energy caused by the variation (17) of properties $\delta \boldsymbol{\mathcal{S}}$. Since we have replaced the array of inclusions by its effective tensor $\boldsymbol{\mathcal{S}}_*(m)$ that continuously depends on δm, we can compute the variation of the cost using the classical variational of stationary conditions: There is no need to consider the continuity conditions on the boundary of the inclusions because they are already taken into account when the tensor of effective properties $\delta \boldsymbol{\mathcal{S}}$ is introduced. Instead, we consider the standard variation of the infinitesimal volume fraction $\delta m(x)$:

$$\delta m(x) = \begin{cases} \mathcal{O}(\epsilon), & \text{if } \|x - x_0\| < \epsilon, \\ 0, & \text{if } \|x - x_0\| \ge \epsilon. \end{cases} \quad \delta m \in C^1(\Omega) \quad (18)$$

and the corresponding stationary optimality conditions.

Remark 3 Tensor $\delta \boldsymbol{\mathcal{S}}$ depends on two parameters of variation: The angle between the layers and the relative elongation α. In the next calculations, we assume that the axes of the tensor $\delta \boldsymbol{\mathcal{S}}$ in base (8) (see (13)) are codirected with the principal axes of matrix $\boldsymbol{\sigma}$. Later, in Section 6 it will be clear that the obtained necessary conditions are the strongest ones, thus justifying this assumption. Namely, we will observe that final results coincide with the extension obtained from sufficient conditions (bounds).

3.3 Increment

The cost consists of the increment of energy due to the variation of $\delta \boldsymbol{\mathcal{S}}$ and the *direct cost* of the variation (i.e., the change in the total cost due to change of quantities of the materials used). When replacing the host material $\boldsymbol{\mathcal{S}}_h$ (with the specific cost γ_h) is replaced with the material of $\boldsymbol{\mathcal{S}}_n$ (with the specific cost γ_n), the direct cost is proportional to the difference of the costs of these materials:

$$(\gamma_n - \gamma_h)\, \delta m. \quad (19)$$

The increment of the energy δ_{E} can be computed as:

$$\delta_{\mathsf{E}}(\alpha) = \mathbf{s}^{\mathbf{T}} \boldsymbol{\mathcal{V}}(\alpha) \mathbf{s} \delta m + G0(\delta m). \quad (20)$$

where $\boldsymbol{\mathcal{V}}$ is given in (17).

Remark 4 Notice that we consider a weak (stationary) variation of the effective properties $\delta \boldsymbol{\mathcal{S}}$ in contrast with the strong variations of the point-wise properties on the boundary of the inclusions in the array. The weak variation of the properties is easy to compute: the stress fields remain constant since the main term of the variation of order of δm is independent of their variations. This remark justifies the use of effective tensors in the variations.

Increment δ_{E} depends on parameter α. We obtain the following expression for $\delta_{\mathsf{E}}(\alpha)$ using (17):

$$\delta_{\mathsf{E}}(\alpha) = \Big(\mathsf{V}_{11}\mathsf{s}_1^2 + \mathsf{V}_{22}\mathsf{s}_2^2 + \mathsf{V}_{33}\mathsf{s}_3^2 + 2\mathsf{V}_{12}\mathsf{s}_1\mathsf{s}_2 + 2\mathsf{V}_{13}\mathsf{s}_1\mathsf{s}_3 + 2\mathsf{V}_{23}\mathsf{s}_2\mathsf{s}_3 \Big) \delta m, \quad (21)$$

and the components of V depend on α as follows

$$V_{11} = \frac{(\mu_h - \mu_n)(\kappa_n(2\kappa_h + \mu_h) + \kappa_h\mu_h)(\kappa_h + \mu_h)}{2\mu_h K(\alpha)}$$

$$V_{13} = \frac{(2\alpha - 1)(\mu_h - \mu_n)(\kappa_n - \kappa_h)(\kappa_h + \mu_h)}{2K(\alpha)}$$

$$V_{22} = \frac{1}{2}\frac{\mu_h - \mu_n}{\mu_h\mu_n}$$

$$V_{33} = \frac{(\kappa_h - \kappa_n)(\mu_n(2\mu_h + \kappa_h) + \kappa_h\mu_h)(\kappa_h + \mu_h)}{2\kappa_h K(\alpha)},$$

$$V_{12} = 0, \quad V_{23} = 0$$

where

$$K(\alpha) = C_1\alpha(\alpha - 1) + \mu_n\kappa_n\kappa_h(\kappa_h + 2\mu_h) + \mu_h\kappa_h(\kappa_h + \mu_h)(\mu_n + \kappa_n) + \mu_n\kappa_n\mu_h^2,$$

in which the constant C_1 is equal to

$$C_1 = 2\kappa_h\mu_h(\mu_h - \mu_n)(\kappa_n - \kappa_h).$$

We remind, that the coordinate axes are directed along the principal stresses. Thus, $\mathbf{s} = (\sigma_x \ 0 \ \sigma_y)^T$ is used in the calculations of (21). Finally, the cost of the variation, $\delta\mathcal{J}\delta m$, is expressed as an explicit function of α:

$$\delta\mathcal{J}\delta m = (\gamma_n - \gamma_h + \delta_{\mathsf{E}}(\alpha))\,\delta m. \tag{22}$$

Since all variations (including the most sensitive one) lead to the nonnegative increment $\delta\mathcal{J}$, the optimality condition of the ith material becomes:

$$\delta\mathcal{J}(\boldsymbol{\mathcal{S}}_i, \boldsymbol{\mathcal{S}}_j, \boldsymbol{\sigma}_j) = \gamma_n - \gamma_h + \min_\alpha \delta_{\mathsf{E}}(\alpha) \geq 0, \tag{23}$$

where $\delta\mathcal{J}(\boldsymbol{\mathcal{S}}_i, \boldsymbol{\mathcal{S}}_j, \boldsymbol{\sigma}_i)$ is a variation caused by adding material $\boldsymbol{\mathcal{S}}_j$ into the material $\boldsymbol{\mathcal{S}}_i$, and $\boldsymbol{\sigma}_i$ is the field in the host material $\boldsymbol{\mathcal{S}}_i$.

3.3.1 The Most Sensitive Variations

The calculation of the optimal variation is slightly different in the case of well- and badly ordered materials. Let us number the materials so that $\mu_1 < \mu_2$. The well-ordered case corresponds to the moduli κ of materials so that $\kappa_1 < \kappa_2$; otherwise, it is called badly ordered case. We demonstrate calculations of the well-ordered case hereafter unless otherwise stated.

According to (23), the optimal increment in energy is

$$\mathfrak{f}_0 = \min_\alpha \delta_{\mathsf{E}}(\alpha). \tag{24}$$

Here the inner parameter α is used to adjust the structure to the acting stress field. To compute an optimal variation, we take the derivative of $\delta_{\mathsf{E}}(\alpha)$ with respect to α in (24), and obtain the following values of α's as zeros of $\dfrac{\partial\delta_{\mathsf{E}}(\alpha)}{\partial\alpha}$:

$$\alpha_1 = -\frac{\sigma_x(\kappa_h + \mu_n)\mu_h + \sigma_y(\kappa_h + \mu_h)\mu_n}{\kappa_h(\sigma_x - \sigma_y)(\mu_n - \mu_h)}, \tag{25}$$

$$\alpha_2 = \frac{\sigma_x(\mu_h + \kappa_n)\kappa_h - \sigma_y(\kappa_h + \mu_h)\kappa_n}{\mu_h(\sigma_x + \sigma_y)(\kappa_h - \kappa_n)}. \tag{26}$$

The optimal values of α must belong to the interval of $[0, 1]$. If none of the (25) and (26) belongs to $(0, 1)$, the optimal values are at the end points, i.e., $\alpha = 0$ or $\alpha = 1$. There are two cases to consider depending on the sign of $\kappa_h - \kappa_n$. Increment $\mathfrak{f}_0$ is defined as $\mathfrak{f}_0^a$ and $\mathfrak{f}_0^b$ for the corresponding cases:

Case A: If $\mu_h - \mu_n > 0$, then $\mathfrak{f}_0$ is

$$\mathfrak{f}_0^a = \begin{cases} \mathsf{E}(0) & \text{if } \dfrac{\sigma_y}{\sigma_x} > \mathfrak{K}, \\ \mathsf{E}(\alpha_2) & \text{if } \dfrac{1}{\mathfrak{K}} \leq \dfrac{\sigma_y}{\sigma_x} \leq \mathfrak{K}, \\ \mathsf{E}(1) & \text{if } \dfrac{\sigma_y}{\sigma_x} < \dfrac{1}{\mathfrak{K}}, \end{cases} \tag{27}$$

when $\kappa_h - \kappa_n > 0$. Here

$$\mathfrak{K} = \frac{(\kappa_n + \mu_h)\kappa_h}{(\kappa_h + \mu_h)\kappa_n} > 1. \tag{28}$$

Case B: If $\mu_h - \mu_n < 0$, then optimal value α_0 always belongs to the boundary of the interval $[0, 1]$. The minimal δ_{E} is reached at the end points, i.e., α_0 is either 0 or 1.

$$\mathfrak{f}_0^b = \begin{cases} \mathsf{E}(1) & \text{if } \sigma_x \leq \sigma_y, \\ \mathsf{E}(0) & \text{if } \sigma_x \geq \sigma_y, \end{cases} \tag{29}$$

when $\kappa_h - \kappa_n < 0$ for which $\mathfrak{K} < 1$.

Note that these cases correspond to physically different situations under the given conditions: Case A corresponds to inclusions of a strong material added to a weak material and Case B corresponds to the inverse situation. The next section will illustrate this point using a specific example.

3.4 Necessary Conditions

Let us determine the regions of permitted fields for an optimal design using the Weierstrass variations or the conditions (27) - (29).

1. Suppose that an inclusion of second material $\boldsymbol{\mathcal{S}}_2$ (strong material) is placed into domain Ω_1 (weak material). The corresponding increment $\delta\mathcal{J}(\boldsymbol{\mathcal{S}}_1, \boldsymbol{\mathcal{S}}_2, \boldsymbol{\sigma}_1)$ is defined by (23):

$$\delta\mathcal{J}(\boldsymbol{\mathcal{S}}_1, \boldsymbol{\mathcal{S}}_2, \boldsymbol{\sigma}_1) = \gamma_2 - \gamma_1 + \mathfrak{f}_0^b(\boldsymbol{\mathcal{S}}_1, \boldsymbol{\mathcal{S}}_2, \boldsymbol{\sigma}_1) \geq 0, \quad (30)$$

where $\boldsymbol{\sigma}_1$ is the field at a point of domain Ω_1 of the first material. Since $\boldsymbol{\mathcal{S}}_1$ and $\boldsymbol{\mathcal{S}}_2$ are given, the inequality in (30) depends only on the stress field $\boldsymbol{\sigma}_1$. The set of stresses $\boldsymbol{\sigma}_1$ that satisfies the condition (30) is called $\mathfrak{F}_1$. If $\boldsymbol{\sigma}_1 \in \mathfrak{F}_1$, material $\boldsymbol{\mathcal{S}}_1$ is optimal. [1]

2. When the inclusion of first material Ω_1 (weak material) is placed into domain Ω_2 (strong material), the increment is defined by (23)

$$\delta\mathcal{J}(\boldsymbol{\mathcal{S}}_2, \boldsymbol{\mathcal{S}}_1, \boldsymbol{\sigma}_2) = \gamma_1 - \gamma_2 + \mathfrak{f}_0^a(\boldsymbol{\mathcal{S}}_2, \boldsymbol{\mathcal{S}}_1, \boldsymbol{\sigma}_2) \geq 0, \quad (31)$$

where $\boldsymbol{\sigma}_2$ is the field at a point of domain Ω_2. The set of stresses $\boldsymbol{\sigma}_2$ that satisfies the condition (31) is called $\mathfrak{F}_2$. If $\boldsymbol{\sigma}_2 \in \mathfrak{F}_2$, then the material $\boldsymbol{\mathcal{S}}_2$ is optimal (see footnote (1)).

Remark 5 When the increment due to the inclusion of the strong material into the weak material is calculated, the formula in (17) is modified as:

$$\delta\boldsymbol{\mathcal{S}} = -\mathbf{V}\delta m + \mathrm{o}(\delta m), \quad \mathbf{V} = \left((\boldsymbol{\mathcal{S}}_2 - \boldsymbol{\mathcal{S}}_1)^{-1} + \boldsymbol{\Delta}\right)^{-1}$$

while subscript $_h$ in (15) becomes: $h = 1$.

The union $\mathfrak{F} = \mathfrak{F}_1 \cup \mathfrak{F}_2$ of two sets of optimality of the first and second materials does not coincide with the whole range of $\boldsymbol{\sigma}$. The remaining part, $\mathfrak{F}_f$, is called the *forbidden region*. Here, none of the materials is optimal. Fields in an optimal design should never belong to this region to matter what the external loading is.

If the external loading belongs to $\mathfrak{F}_f$, the pointwise fields are still in their regions $\mathfrak{F}_1$ and $\mathfrak{F}_2$, but the mean field matches the external load. This phenomenon is the reason of formation a structure or a composite material in the optimal designs.

Remark 6 According to the theory of quasiconvexity, the solution (stress field) of the variational problem (6) is oscillatory if the Lagrangian (2) is not *quasiconvex*, see for example Cherkaev (2000). The forbidden region $\mathfrak{F}_f$ necessarily belongs to the region where the Lagrangian is not quasiconvex.

[1] Optimality is understood in the sense of satisfaction of necessary conditions.

Remark 7 Dealing with special necessary conditions, one cannot guarantee that there are no other tests that are more restrictive. If this were the case, the forbidden region would be larger than $\mathfrak{F}_f$. For the considered problem, however, the results are final as it follows from the results of Section 6.

Details of the calculations are shown explicitly next when $\sigma_x\sigma_y > 0$. Assume that the axes are oriented so that $\sigma_{xy} = 0$. In this case, σ_x and σ_y become the eigenvalues of $\boldsymbol{\sigma}$. The set $\mathfrak{F}_1$ of stresses optimal in the material $\boldsymbol{\mathcal{S}}_1$ and set $\mathfrak{F}_2$ of stresses optimal in $\boldsymbol{\mathcal{S}}_2$ are determined by (30) and (31), respectively:

$$\mathfrak{F}_1 = \{\boldsymbol{\sigma}_1 \mid \delta\mathcal{J}(\boldsymbol{\mathcal{S}}_1, \boldsymbol{\mathcal{S}}_2, \boldsymbol{\sigma}_1) = \gamma_1 - \gamma_2 + \mathsf{E}(1) \geq 0\}. \quad (32)$$

$$\mathfrak{F}_2 = \left\{\boldsymbol{\sigma}_2 \mid \delta\mathcal{J}(\boldsymbol{\mathcal{S}}_2, \boldsymbol{\mathcal{S}}_1, \boldsymbol{\sigma}_2) = \gamma_2 - \gamma_1 + \left\{\begin{array}{ll} \mathsf{E}(0) & \text{if } \frac{\sigma_y}{\sigma_x} < \mathfrak{K}, \\ \mathsf{E}(\alpha_2) & \text{if } \frac{\sigma_y}{\sigma_x} \geq \mathfrak{K}, \end{array}\right\} \geq 0 \right\} \quad (33)$$

where

$$\mathsf{E}(\alpha_2) = -\frac{1}{4}\frac{(\kappa_1 - \kappa_2)(\kappa_2 + \mu_2)}{\kappa_2(2\kappa_1\kappa_2 + \kappa_1\mu_2 + \kappa_2\mu_2)}(\sigma_x + \sigma_y)^2. \quad (34)$$

When $\sigma_x\sigma_y < 0$, parameter α_1 lies in the interval of (0,1). Therefore, $\mathsf{E}(\alpha_2)$ is replaced by $\mathsf{E}(\alpha_1)$ in (33) which yields to the expression:

$$\mathsf{E}(\alpha_1) = -\frac{1}{4}\frac{(\mu_1 - \mu_2)(\kappa_2 + \mu_2)}{\mu_2(2\mu_1\mu_2 + \kappa_2\mu_1 + \kappa_2\mu_2)}(\sigma_x - \sigma_y)^2. \quad (35)$$

The obtained results can be interpreted for the condition of $\sigma_x\sigma_y > 0$ as follows:

- Formula (32) corresponds to the variation when the inclusion of the *strong material* is implanted into a *weak material.* The most sensitive variation corresponds to a fillet (laminates) that is placed along the direction of maximal field. Thus, the nuclei "exposes itself" to the maximal effect of the variation.

- Formula (33) corresponds to the variation when the inclusion of the *weak material* is implanted into the *strong material.* The most sensitive variation corresponds either to the family of nuclei in the second rank lamination (if the ratio of σ_x and σ_y is smaller that a limit value) or a fillet (if the ratio of σ_x and σ_y is larger than this value). Thus, the weak material "hides itself" to maximize the effects of the variation.

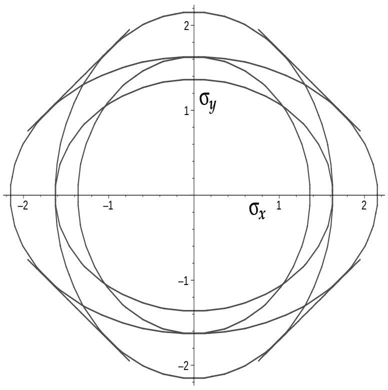

Fig. 2 The stress fields when the materials have zero Poisson ratio.

4 Results

4.1 Range of Admissible Fields

Based on the results of Section 3.3.1, we observe that the boundaries of $\mathfrak{F}_1$ and $\mathfrak{F}_2$ consist of the two following components: Two symmetric curves

$$\mathsf{E}(\alpha) = \begin{cases} A\sigma_x^2 + B\sigma_y^2 + 2C\sigma_x\sigma_y = 1 \\ B\sigma_x^2 + A\sigma_y^2 + 2c\sigma_x\sigma_y = 1 \end{cases} \quad (36)$$

where the constant coefficients A, B and C are determined by the material constants; this component corresponds to optimal values $\alpha = 0$ or $\alpha = 1$ of $\mathsf{E}(\alpha)$. The other component is represented by two families of straight lines

$$\mathsf{E}(\alpha_i) = \begin{matrix} D_1(\sigma_x + \sigma_y)^2 = 1 \\ D_2(\sigma_x - \sigma_y)^2 = 1 \end{matrix} \quad (37)$$

where the constant coefficients D_1 and D_2 are determined by the material constants; this component corresponds to stationary values of α in (25) and (26).

Well-ordered case: In this case, the curves in (36) are ellipses since $A > 0$, $B > 0$, and $AB > C^2$. The optimality regions are presented in Figure 2 and Figure 3. Region $\mathfrak{F}_1$ of optimality of the weak and cheap material lies inside of intersection of two smaller ellipses; this region is shown in Figure 3 by the curve with crosses on it. Region $\mathfrak{F}_2$ of optimality of the strong and expensive material lies outside of the linear envelope stretched on two larger ellipses; this region is shown by the curve with circles on it. The boundary contains elliptical and straight components. Forbidden region $\mathfrak{F}_f$ lies between $\mathfrak{F}_1$ and $\mathfrak{F}_2$. In Figure 3(a), we first plot the curves determined by stationary values 0, 1, α_1, and α_2 of α, using

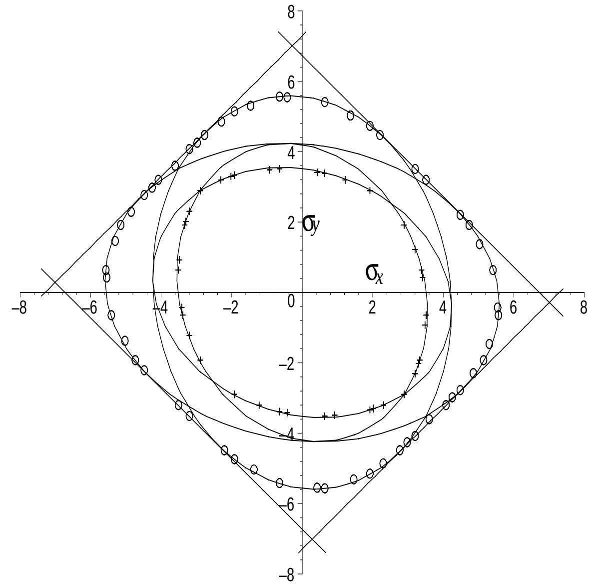

(a) Region $\mathfrak{F}_1$ lies inside of the region given by crosses, while region $\mathfrak{F}_2$ lies outside of the region given by circles. The forbidden region $\mathfrak{F}_f$ lies between the regions.

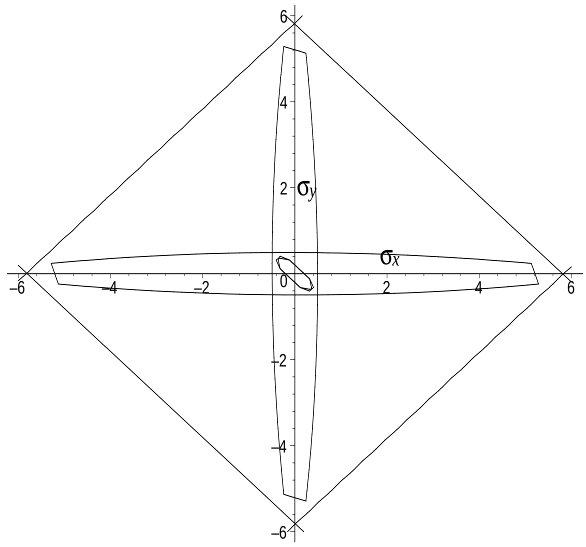

(b) The asymptotic case when the ratio between the material properties is large.

Fig. 3 Optimal fields for well-ordered case: $\kappa_1 < \kappa_2$ and $\mu_1 < \mu_2$.

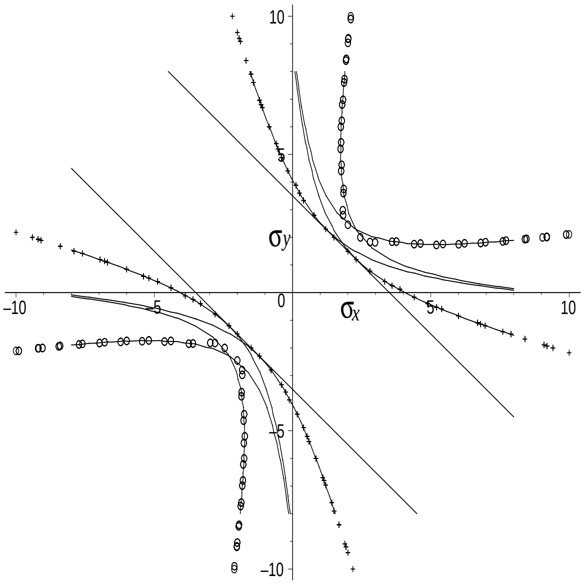

(a) Region $\mathfrak{F}_1$ lies inside of the region given by crosses, while region $\mathfrak{F}_2$ lies outside of the region given by circles, and in between lies the forbidden region $\mathfrak{F}_f$.

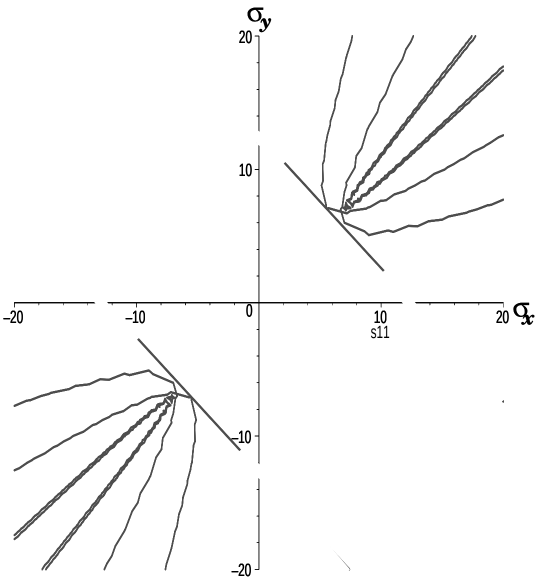

(b) The asymptotic case when the ratio between the material properties is large.

Fig. 4 Optimal fields for badly ordered case: $\kappa_1 > \kappa_2$ and $\mu_1 < \mu_2$.

(25) (26). Next, we follow the conditions in Section 3.4 to select among these stationary values.

In Figure 3(b), the asymptotic case is shown. One of the materials has infinite compliance or becomes void and the optimization problem becomes the problem of *topology optimization* Bendsøe (1995). The region of optimality $\mathfrak{F}_1$ of the void "material" shrinks to zero as expected. Elliptic components of the boundary of $\mathfrak{F}_2$ disappear.

Finally, we observe that ellipses in Figure 3 are rotated by angles depending on Poisson ratio (e.g., when Poisson ratio is zero, $C = 0$ in (36), see Figure 2 where the ellipses are mutually orthogonal).

Badly ordered case: In the badly ordered case, A and B in (36) have different signs, and the elliptical components of the boundaries in well-ordered case become hyperbolic. The situation is more tedious than in the well-ordered case. Each material plays both a role of *strong* or *weak* one, depending on the type of field $\boldsymbol{\sigma}$: If the field is close to hydrostatic, the ordering of the bulk moduli defines what material is called *strong* or *weak* and if the field is close to shear, the ordering of the shear moduli defines the ordering of materials. The cheaper material is always optimal in the proximity of the origin (that corresponds to small magnitude of the stress).

The results are presented at Figure 4(a). The boundary of the region of optimality for the more expensive material corresponds to the intersection of two sharp hyperbolas in (36); this region is shown by a curve with circles on it.

The boundary of the region of optimality for the cheaper material corresponds to the convex envelope stretched on two other hyperbolas; this region is shown by a curve with crosses. The straight part of the envelope corresponds to optimality of implant that is formed as a second-rank dilute composite.

When the cost of both materials is the equal, the regions degenerates. One can verify that all boundaries become straight lines passing through the origin.

Optimal fields and optimal structures We already mentioned that the optimal design problem we are dealing with was investigated in a number of papers. Particularly, it was found that the variety of optimal structures consists of second-rank laminates. Also, the Vigdergauz structures are equally optimal if $\sigma_x\sigma_y > 0$ and one of the phases is void.

Our analysis allows us to explain the optimality of these different geometries. Suppose that a periodic optimal structure is submerged into a constant external stress field $\boldsymbol{\sigma}$. If the external field belongs to the forbidden region $\mathfrak{F}_f$, the local fields belong to the boundaries of the permitted regions, $\mathfrak{F}_1$ or $\mathfrak{F}_2$, and the averaged stress is equal to the applied one.

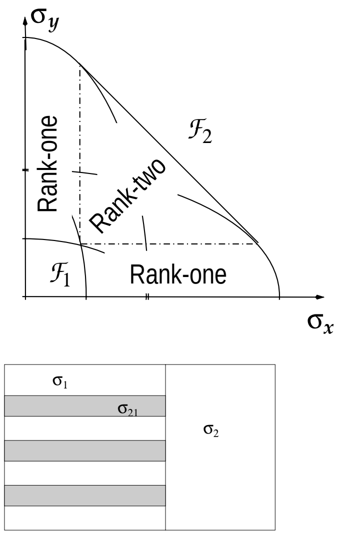

Fig. 5 The stress fields when the materials have zero Poisson ratio: Case when det $\boldsymbol{\sigma} \geq 0$.

The second-rank laminates are optimal, if the external field belongs to the triangle "Rank-two" in Figure 5, that allows the representation

$$\boldsymbol{\sigma} = m_1\boldsymbol{\sigma}_1 + m_2\boldsymbol{\sigma}_{21} + m_3\boldsymbol{\sigma}_2 \tag{38}$$

where $m_i \geq 0, \; m_1 + m_2 + m_3 = 1$. Here, stress $\boldsymbol{\sigma}_1$ corresponds to the first (weak) material located in the inner layer of the second-rank structure, and it belongs to the corner point of the boundary of its permitted region: $\boldsymbol{\sigma}_1 = \pm\boldsymbol{\sigma}_2$, see Figure 5. In (38), stress $\boldsymbol{\sigma}_{21}$ corresponds to the second (strong) material located in the other inner layer of the second-rank structure. The fields $\boldsymbol{\sigma}_1$ and $\boldsymbol{\sigma}_{21}$ are compatible $\det(\boldsymbol{\sigma}_1 - \boldsymbol{\sigma}_{21}) = 0$. This field corresponds to that point of the boundary of permitted region $\mathfrak{F}$ where the elliptical component meets the straight component (see Figure 5). Finally, stress $\boldsymbol{\sigma}_2$ corresponds to the second (strong) material located in the outer layer of the second-rank structure. This field is not compatible with neither $\boldsymbol{\sigma}_1$ nor $\boldsymbol{\sigma}_{21}$ but it is compatible with their weighted sum: $\det(\boldsymbol{\sigma}_s - \boldsymbol{\sigma}_2) = 0$ where $\boldsymbol{\sigma}_s = m_1/(m_1 + m_2)\boldsymbol{\sigma}_1 + m_2/(m_1 + m_2)\boldsymbol{\sigma}_{21}$. This field corresponds to a point the straight component of the boundary of region $\mathfrak{F}$ (see Figure 5).

Simple laminates are optimal when the external field is anisotropic, and belongs to curved trapezoids "Rank-one" in Figure 5: It combines as a sum of two fields; each of them belong to the elliptical component of the boundary of the correspondent permitted region and they are compatible.

The fields in Vigdergauz structures or in Hashin-Shtrikman "coated spheres" are different, however they also belong to the boundaries of the permitted regions. The field in the nucleus again belongs to the corner point of its permitted region, being isotropic: $\sigma_x = \sigma_y$. The fields in the envelope vary from point to point, but they remain on the straight component of the boundary of $\mathfrak{F}_2$!

Here, we do not demonstrate the bulky calculations that confirm these results; the reader can check them using the formulas in the previous section.

Remark 8 The optimality of the mentioned structures was independently verified by the sufficient conditions. This optimality now proves that our variations are the most sensitive ones. Indeed, if a more sensitive variation existed, it would correspond to a larger forbidden region; the fields in mentioned structures would be in that larger region and therefore would be nonoptimal which contradicts sufficient conditions.

Structures with infinitesimal elements The optimality requirements force the fields to obey an additional condition: they must belong to the boundaries of the permitted regions if the external field is in the forbidden region. This requirement cannot be enforced in a "bulky" domain filled with one material since we can control only the curve that divide the domains of different material. Therefore, we conclude that the optimal structure should, in general, not contain "bulky domains" that a dividing curve should have infinitely often wiggles, Cherkaev (2000), unless the structure is strictly periodic and the load is strictly constant. The optimal structure becomes a composite in which fields belong to the boundaries ($\mathfrak{F}_1 = constant_1$) or ($\mathfrak{F}_2 = constant_2$) at each point (see Table (1)).

4.2 Norms

For centuries, architects and engineers knew that stress fields should be distributed evenly over an optimal structure; thus the overstressed regions require more reinforcements, while the understressed regions can be lightened. This common sense requirement of optimality of equally stressed designs can be stated mathematically in terms of a norm of a stress field.

We consider the well-ordered case. Our results can be rewritten in the following form: The boundaries of $\mathfrak{F}$ correspond to constancy of two norms:

Table 1 Table of the optimal design.

Average field $\boldsymbol{\sigma}_0$	Optimal Material
$\boldsymbol{\sigma}_0 \in \mathfrak{F}_1$	*Material 1*
$\boldsymbol{\sigma}_0 \in \mathfrak{F}_2$	*Material 2*
$\boldsymbol{\sigma}_0 \in \mathfrak{F}_f$	Composite in which $\boldsymbol{\sigma}_1 \in \partial\mathfrak{F}_1$ and $\boldsymbol{\sigma}_2 \in \partial\mathfrak{F}_2$ everywhere

$$\mathcal{N}_1(\boldsymbol{\sigma}_1) = \sqrt{\mathsf{E}(1)}, \qquad \text{and}$$

$$\mathcal{N}_2(\boldsymbol{\sigma}_2) = \begin{Bmatrix} \sqrt{\mathsf{E}(0)} & \text{if } \dfrac{\sigma_y^2}{\sigma_x^2} < \mathfrak{K}, \\ \sqrt{\mathsf{E}(\alpha_2)} & \text{if } \dfrac{\sigma_y^2}{\sigma_x^2} \geq \mathfrak{K}, \end{Bmatrix} \tag{39}$$

where $\boldsymbol{\sigma}_1 = \begin{pmatrix} \sigma_x^1 & 0 \\ 0 & \sigma_y^1 \end{pmatrix}$ is the stress field in Ω_1, and $\boldsymbol{\sigma}_2 = \begin{pmatrix} \sigma_x^2 & 0 \\ 0 & \sigma_y^2 \end{pmatrix}$ is the stress field in Ω_2; and $\mathfrak{K}$ is given in (28).

In (39), $\mathsf{E}(0)$ and $\mathsf{E}(1)$ are given in (36), and $\mathsf{E}(\alpha_2)$ is given in (37).

The reader can check that $\mathcal{N}_1$ and $\mathcal{N}_2$ are indeed rotationally invariant norms of two-by-two symmetric tensors: The axioms of norms are satisfied. In the one-dimensional case, both $\mathcal{N}_1$ and $\mathcal{N}_2$ degenerate to the absolute value of the stress.

In the regions where composites are used these norms are constant in each material in an optimal structure

$$\mathcal{N}_1 \leq constant_1, \quad \text{or } \mathcal{N}_2 \geq constant_2. \tag{40}$$

The mean field varies due to the variation of concentrations. The mixtures should be infinitesimal fine, otherwise one cannot preserve the constancy of the norm inside the solid region of a material.

Remark 9 Notice that the equation (40) is fulfilled everywhere in the design domain. These conditions are satisfied as equalities in the whole region of composites. The conditions are nonlocal: the variation of the loading in a small subdomain leads to an evenly distributed variation of optimal fields and corresponding optimal microstructures in all design domain. This feature, natural for optimal design, is a mark of *quasiconvex envelope*, see Cherkaev (2000) since the Euler-Lagrange equations of the corresponding variational problem lose ellipticity that is the reason for localization.

Topology optimization Finally, we observe that in the asymptotic case when one of the materials is void (the case of *topology optimization*, see Figure 3(b), the small ellipses in the center become a point at the origin: $\mathcal{N}_1 = 0$. The non-void material must be never understressed in an optimal design: Its norm becomes $\mathcal{N}_2 = |\sigma_x| + |\sigma_y|$ and the inequality holds

$$\mathcal{N}_2 \geq \sqrt{\frac{8\mu_2\kappa_2(\gamma_2 - \gamma_1)}{\mu_2 + \kappa_2}}, \quad \forall x \in \Omega_2. \tag{41}$$

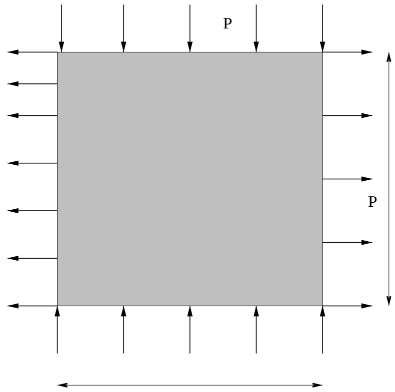

Fig. 6 Plate design domain, load and boundary conditions.

5 Analyzer

The obtained necessary conditions can be used to quantitative examine *suboptimal projects*.

A design may have stresses whose norm is quite close to a constant everywhere. This design would approximately solve the optimality conditions and therefore would be suboptimal. The geometry of the design structure can be arbitrary; only the fields in it need to be checked. The necessary conditions provide a tool that we call an *analyzer* to examine the given structure and to judge how close to an optimal one is it.

Using the *analyzer*, we can see how far from the constancy is the corresponding norm of the stress field. The use of it is similar to the use of color maps of a failure criterion that show how close the stresses are to the limit.

5.1 An example

We illustrate the use of the *analyzer* by the following example. Consider a plane domain, a 25cm×25cm plate with Poisson ratio 0.32 and Young's modulus 1e; the plate is loaded as shown in Figure 6. The caverns of unknown shape will be introduced and the results will be compared using the *analyzer*. We deal with an asymptotic case where one of the materials is void, or with the problem of topology optimization. Another application of this problem can be seen in Küçük (2001) where a plate for a circle, square and two rectangles is examined with different material properties.

In this case, it is expected that $\mathcal{N}_1 = 0, \mathcal{N}_2 = |\sigma_x| + |\sigma_y|$; the norm $\mathcal{N}_2$ must be constant everywhere in an optimal projection if $\sigma_x\sigma_y > 0$, that trace of tensor $\boldsymbol{\sigma}$ is constant, and if $\sigma_x\sigma_y < 0$, then Von Mises stress is constant (see Section 4.2). This corresponds to the earlier results of Bendsøe (1995); Grabovsky (1996b). We consider examples of suboptimal design for planar structures, and compare the shapes of a circle, square and

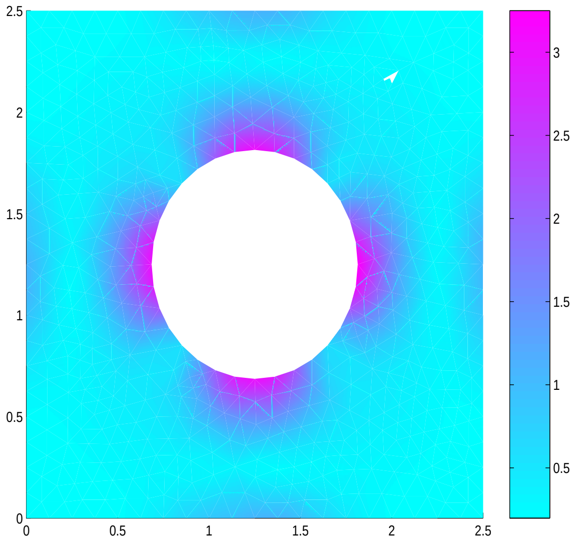

Fig. 7 Von Mises stress distribution for a deformed structure when a circle is included.

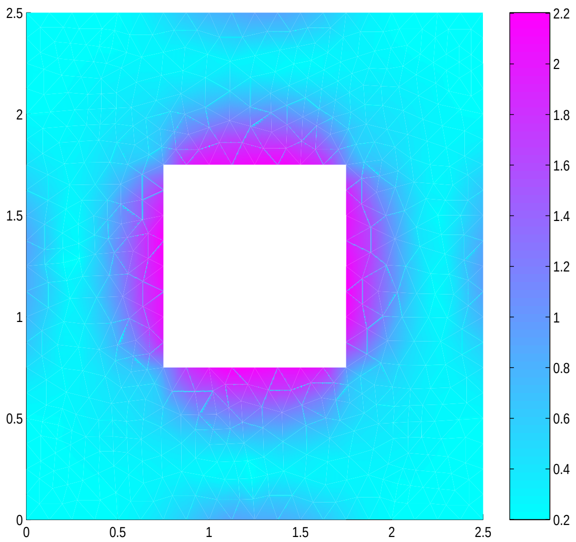

Fig. 8 Von Mises stress distribution for a deformed structure when a combination of different geometries is included.

four ellipses with the same areas, following the ideas of Cherkaev et al. (1998a).

We find that the structure in Figure 9 better approximates the necessary conditions than the others. Comparing this norm in Figure 8-Figure 9 for various structures, we observe that the deviation from the constancy of the norm $\mathcal{N}(\boldsymbol{\sigma})$ is smaller in Figure 9 than the others. It is not claimed to be the optimal but it represents a reasonable suboptimal design. In the *true optimal* solution the norm $\mathcal{N}(\boldsymbol{\sigma})$ is expected to be constant everywhere.

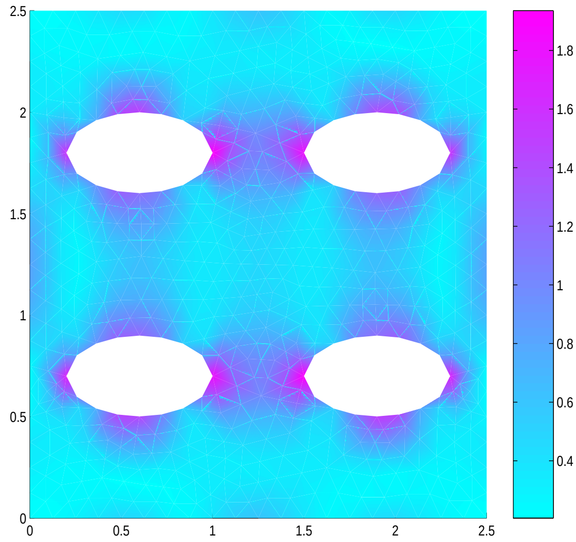

Fig. 9 Von Mises stress distribution for a suboptimal structure.

We obtain the following normalized energies $\mathcal{W}$ for each structure in Figure 7-Figure 9; $\mathcal{W} = 0.3967$ in Figure 7, $\mathcal{W} = 0.3508$ in Figure 8, and $\mathcal{W} = 0.2523$ in Figure 9. This calculation confirms that that the structure in Figure 9 is the best from the compared set.

Checking the norms given in (39) allows us to describe quantitatively suboptimal structures and to point to the places where the norm derivated from the constant. One can use this as a tool to decide if a structure is close to optimal.

6 Supplement: Comparison with Sufficient Conditions

6.1 Translation method

The analysis of admissible regions is based on special necessary conditions; in principle, these regions could be decreased by more sophisticated conditions. Here we show that in fact the results cannot be improved, by comparing necessary conditions and sufficient conditions.

The sufficient conditions obtained by the Translation method (see the discussion of the method and its development in the books Cherkaev and Kohn (1997), Cherkaev (2000), and Milton (2001)) are used here to derive the information of the admissible regions. Contrary to necessary conditions, the sufficient conditions correspond to admissible regions that could, in principle, be abridged by more sensitive conditions. Both methods provide the two-side bounds for admissible regions.

In setting of two-dimensional elasticity, the translation method exploits the nonuniqueness of the definition of the elastic moduli, see Cherkaev et al. (1992). This nonuniqueness allows us to consider the "translated" tensor of elastic moduli instead of the original tensor and bound this new tensor by the harmonic mean bound. Then the parameter of the translation is adjusted to make the bound stronger. The elasticity tensors $\boldsymbol{\mathcal{S}}$ are translated by using a multiple of a special tensor $\boldsymbol{\mathcal{T}}$ called *translator*,

$$\boldsymbol{\mathcal{S}}^{trans} = \boldsymbol{\mathcal{S}} - t\boldsymbol{\mathcal{T}}, \tag{42}$$

where t is a constant. Formally, the translator is the isotropic tensor of two-dimensional elasticity with opposite bulk and shear moduli: $\kappa_{\boldsymbol{\mathcal{T}}} = 1$ and $\mu_{\boldsymbol{\mathcal{T}}} = -1$.

The mentioned nonuniqueness leads to the following property: the stress field of any periodic structure loaded by homogeneous external forces at infinity stays the same if the elasticity tensors $\boldsymbol{\mathcal{S}}_i$ are replaced by $\boldsymbol{\mathcal{S}}_i^{trans}$ no matter what the magnitude t of the translator is, providing that the translated tensors $\boldsymbol{\mathcal{S}}_i^{trans}$ are positive definite;

$$\boldsymbol{\mathcal{S}}_i - t\boldsymbol{\mathcal{T}} \geq 0 \quad \forall i. \tag{43}$$

6.2 Basic formulas

In order to compare necessary conditions with the translation method, we need to compute the fields in the structures predicted by this method. Earlier a similar problem was considered in Grabovsky (1996a) and it is discussed in Cherkaev (2000); Milton (2001).

Relaxation of the problem in (7) is based on the following essentially algebraic procedure: Consider the Lagrangian in (6) and neglect all differential constraints on the stress field. Then the stress tensor become constant in each material, since the energy of each well is convex. The minimization problem (6) becomes an algebraic problem

$$\mathcal{C}(\mathsf{F}) = \min_{\boldsymbol{\sigma} \in \mathcal{F}_0^s(x)} [\mathsf{F}(\boldsymbol{\sigma}) + \gamma_1 m_1 + \gamma_2 m_2], \tag{44}$$

where

$$\mathsf{F}(\boldsymbol{\sigma}) = \frac{1}{2} \sum_i m_i \boldsymbol{\sigma}_i^T \boldsymbol{\mathcal{S}}_i(x) \boldsymbol{\sigma}_i \tag{45}$$

and

$$\mathcal{F}_0^s(x) = \{\boldsymbol{\sigma}_i |\ G = \sum_i m_i \boldsymbol{\sigma}_i - \boldsymbol{\sigma}_0 = 0\}, \tag{46}$$

$\boldsymbol{\sigma}_i$ is the field in the ith material subject only to integral restrictions (46), and m_i is the fixed fraction of the ith material in the design domain. This lower bound of the energy in (44) is the convex envelope of the Lagrangian $\boldsymbol{\mathcal{G}}$.

Let us compute the fields that solve the problem (44). To minimize F under the constraint (46), we compute

$$\frac{\partial}{\partial \boldsymbol{\sigma}_i}(\mathsf{F} + \lambda G) = m_i(\boldsymbol{\mathcal{S}}_i \boldsymbol{\sigma}_i + \lambda) = 0, \tag{47}$$

where λ is the Lagrange multiplier by (46). From (46) and (47), we find:

$$\lambda = -\overline{\boldsymbol{\mathcal{S}}} \boldsymbol{\sigma}_0, \tag{48}$$

and

$$\boldsymbol{\sigma}_i = \boldsymbol{\mathcal{S}}_i^{-1} \overline{\boldsymbol{\mathcal{S}}} \boldsymbol{\sigma}_0. \tag{49}$$

where

$$\overline{\boldsymbol{\mathcal{S}}} = \left(\sum_i m_i \boldsymbol{\mathcal{S}}_i^{-1} \right)^{-1}.$$

Substituting (49) into (44), we obtain the lower bound that is the convex envelope of the multi-well Lagrangian.

$$\mathcal{C}(\mathsf{F}) = \frac{1}{2} \boldsymbol{\sigma}_0^T \overline{\boldsymbol{\mathcal{S}}} \boldsymbol{\sigma}_0 \leq \mathsf{F}(\boldsymbol{\sigma}) \quad \forall \boldsymbol{\sigma}. \tag{50}$$

The translation method improves the bound by using the nonuniqueness of $\boldsymbol{\mathcal{S}}$ (generally, by using the quasiconvex but not convex functions, see the discussion in Cherkaev (2000)). The formal application of the translation bound is easy: we simply replace the elasticity tensors in (50) and (49) by the translated tensors as in (42), subject to the constraint (43). In order to make this bound effective, we maximize the right-hand side with respect to t; and obtain

$$\mathsf{F}(\boldsymbol{\sigma}) \geq \max_{t:(43)\text{holds}} \frac{1}{2} \boldsymbol{\sigma}_0^T (\boldsymbol{\mathcal{S}}_h + \boldsymbol{\mathcal{T}}) \boldsymbol{\sigma}_0, \tag{51}$$

where

$$\boldsymbol{\mathcal{S}}_h = \overline{\boldsymbol{\mathcal{S}} - \boldsymbol{\mathcal{T}}},$$

$$= \left(\sum_i m_i (\boldsymbol{\mathcal{S}}_i - \boldsymbol{\mathcal{T}})^{-1} \right)^{-1}. \tag{52}$$

Since all involved elasticity tensors correspond to the isotropic elasticity, we replace the elastic moduli:

κ is replaced by $\kappa - t$,
μ is replaced by $\mu + t$

and (43) leads to

$$\mathcal{T} = \{t \mid -\min\{\mu_1, \mu_2\} \leq t \leq \min\{\kappa_1, \kappa_2\}. \tag{53}$$

6.3 Comparing the fields

The obtained formulas assume that the volume fractions in the mixture are fixed. In contrary, the necessary conditions do not deal with volume fractions, only with the cost of materials. To compare the fields in structures, we need to exclude volume fraction m from the formulas for translation bounds by computing the minimum over it. The dependence of the translation parameter t must be excluded as well. This leads to the following problem

$$\boldsymbol{\mathcal{L}}(\mathsf{F}) = \min_m \left\{ \max_{t\in\mathcal{T}} \frac{1}{2}\boldsymbol{\sigma}_0^T(\boldsymbol{\mathcal{S}}_h + \boldsymbol{\mathcal{T}})\boldsymbol{\sigma}_0 + m_1\gamma_1 + m_2\gamma_2 \right\}, \tag{54}$$

where $\boldsymbol{\mathcal{S}}_h$ is given in (52). After the optimal parameters m and t are computed as function of the load $\boldsymbol{\sigma}_0$, these values are used to compute the fields using the translation analog of (49).

The solution of the inner maximization problem in (54) is found from:

$$\frac{\partial \boldsymbol{\mathcal{L}}(\mathsf{F})}{\partial t} = 0, \text{ and } \frac{\partial^2 \boldsymbol{\mathcal{L}}(\mathsf{F})}{\partial t^2} \le 0 \text{ for all } t \in \mathcal{T}. \tag{55}$$

First, assume that optimal values of t belong to the set (53). The conditions in (55) are observed by the following t's as a function of the field

$$t_1 = -\frac{\sigma_x \mathrm{b} - \sigma_y \mathrm{a}}{\sigma_x \mathrm{d} + \sigma_y \mathrm{c}}; \tag{56}$$

$$t_2 = -\frac{\sigma_y \mathrm{b} + \sigma_x \mathrm{a}}{\sigma_x \mathrm{c} + \sigma_y \mathrm{d}}; \tag{57}$$

where

$$\mathrm{a} = \mu_1\kappa_1\kappa_2 - \mu_1\mu_2\kappa_2 - \kappa_1\mu_2\kappa_2 + \mu_1\kappa_1\mu_2,$$

$$\mathrm{b} = \mu_1\mu_2\kappa_2 - \kappa_1\mu_2\kappa_2 + \mu_1\kappa_1\kappa_2 - \mu_1\kappa_1\mu_2,$$

$$\mathrm{c} = \mu_1\kappa_2 - \kappa_1\mu_2, \tag{58}$$

$$\mathrm{d} = 2(-\kappa_1\mu_2 + \mu_1\kappa_1 - \mu_1\kappa_2 + \mu_2\kappa_2)m \tag{59}$$

$$-2\mu_1\kappa_1 + \mu_1\kappa_2 + \kappa_1\mu_2.$$

The correct sense of these extremum points is monitored by the second derivatives

$$\left.\frac{\partial^2 \boldsymbol{\mathcal{L}}(\mathsf{F})}{\partial t^2}\right|_{t=t_1} = -\frac{mA^4(1-m)}{(\sigma_y^2 - \sigma_x^2)(\kappa_2-\kappa_1)(\mu_2-\mu_1)},$$
$$\left.\frac{\partial^2 \boldsymbol{\mathcal{L}}(\mathsf{F})}{\partial t^2}\right|_{t=t_2} = \frac{mA^4(1-m)}{(\sigma_y^2 - \sigma_x^2)(\kappa_2-\kappa_1)(\mu_2-\mu_1)}, \tag{60}$$

where A is a function of the material properties. Notice that in (60) the signs of the second derivatives depend on field $\boldsymbol{\sigma}_0$ and the material properties.

In the *well-ordered* case when it is assumed that $\mu_1 < \mu_2$ and $\kappa_1 < \kappa_2$; we have

$$t_{opt} = \begin{cases} t_1 & \text{if } \sigma_x < \sigma_y, \\ t_2 & \text{if } \sigma_x > \sigma_y. \end{cases} \tag{61}$$

(for the *badly-ordered* case, the roots t_1 and t_2 switch places).

To calculate the optimal values of m, we impose conditions similar to the ones given in (55). Hence, we have

$$m_{t_1} = \frac{2\mu_1\kappa_1(\kappa_2+\mu_2)\mathrm{k} - \sqrt{\mathrm{l}}}{2\mathrm{a}\mathrm{k}} \tag{62}$$

where

$$\mathrm{k} = 2\mathrm{a}(\gamma_1-\gamma_2) - (\kappa_1-\kappa_2)\sigma_x^2 \quad \text{and}$$
$$\mathrm{l} = (\kappa_2+\mu_2)(\kappa_1+\mu_1)(\mathrm{a}\sigma_y - \mathrm{b}\sigma_x)^2\mathrm{k},$$

and the optimal volume fraction corresponding to t_2 is

$$m_{t_2} = \frac{2\mu_1\kappa_1(\kappa_2+\mu_2)\tilde{\mathrm{k}} - \sqrt{\tilde{\mathrm{l}}}}{2\mathrm{a}\tilde{\mathrm{k}}} \tag{63}$$

where

$$\tilde{\mathrm{k}} = 2\mathrm{a}(\gamma_1-\gamma_2) - (\kappa_1-\kappa_2)\sigma_y^2 \quad \text{and}$$
$$\tilde{\mathrm{l}} = (\kappa_2+\mu_2)(\kappa_1+\mu_1)(\mathrm{a}\sigma_x - \mathrm{b}\sigma_y)^2\tilde{\mathrm{k}}.$$

6.4 Asymptotic: Topology optimization

First, we examine the case of topology optimization: $\kappa_1 = \mu_1 = 0$. The case can be examined analytically. In this case, the optimal values of t take only limiting values, see Cherkaev (2000): $t = -\mu_2$ and $t = \kappa_2$.

Case: $t = -\mu_2$ The optimal values m^{μ_2} of m are

$$m^{\mu_2} = \frac{|\sigma_x + \sigma_y|}{4}\sqrt{\frac{2(\kappa_2+\mu_2)}{\kappa_2\mu_2(\gamma_2-\gamma_1)}} \tag{64}$$

The condition $m^{\mu_2} \in [0,1]$ yields to the inequality for the stresses:

$$0 \le |\sigma_x + \sigma_y| \le \sqrt{\frac{8\mu_2\kappa_2(\gamma_2-\gamma_1)}{\mu_2+\kappa_2}}. \tag{65}$$

It shows that the region of optimal fields is bounded by an inclined strip in the plane of eigenvalues σ_x and σ_y.

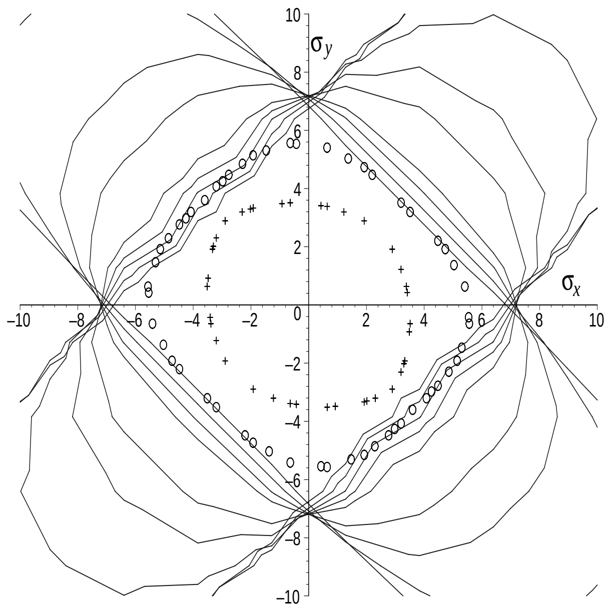

Fig. 10 The bound found from the necessary conditions is approached from above by using the translation bound for $-\frac{1}{2\mu_{max}} < t < \frac{1}{2\kappa_{max}}$.

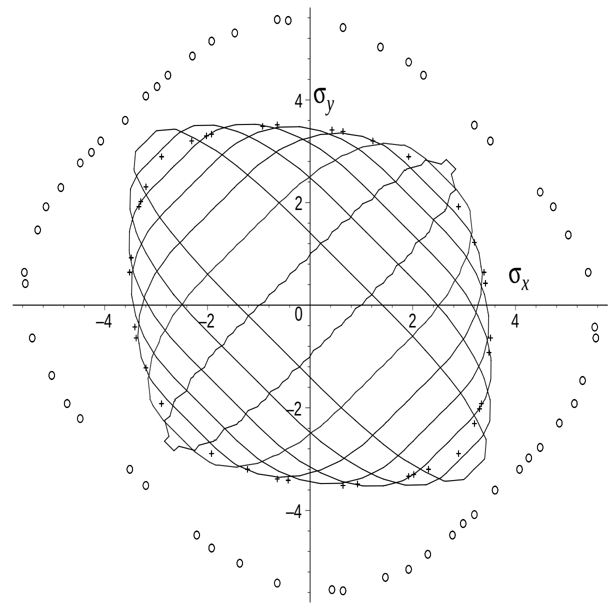

Fig. 11 The bound found from the necessary conditions is approached from below by using the translation bound for $-\frac{1}{2\mu_{max}} < t < \frac{1}{2\kappa_{max}}$.

Case: $t = \kappa_2$ The optimal values m^{κ_2} of m are

$$m^{\kappa_2} = \frac{|\sigma_x - \sigma_y|}{4}\sqrt{\frac{2(\kappa_2 + \mu_2)}{\kappa_2\mu_2(\gamma_2 - \gamma_1)}}. \tag{66}$$

Since $m^{\kappa_2} \in [0, 1]$, the corresponding inequality for σ_x and σ_y is satisfied

$$0 \le |\sigma_x - \sigma_y| \le \sqrt{\frac{8\mu_2\kappa_2(\gamma_2 - \gamma_1)}{\mu_2 + \kappa_2}}. \tag{67}$$

It shows that the region of optimal fields is bounded by an orthogonal inclined strip, too. Two intersections of the two inequalities (65) and (67) define the diamond-like forbidden region.

Remark 10 The inequalities (65) and (67) match the necessary condition (41) that defines the same the diamond-like domain in the plane of eigenvalues. This proves the extreme character of these conditions and, consequently, the extreme character of the used variations. Notice the opposite signs of inequalities in the necessary condition (41) and sufficient conditions; (65) and (67).

6.5 General case

In Figure 10 and Figure 11, we show the fields in the materials according to the Translation bounds. The family of the curves correspond to different values of t. For each fixed value of $t \in T$ the bound of the energy is minimized over m; optimal m is given by (62) and (63) and is subjected to the condition of being in the interval of (0,1). The calculation of the bound was conducted using MAPLE.

One can observe from these figures, how the forbidden region obtained from sufficient conditions matches the region calculated from necessary conditions. For any fixed t the sufficient condition corresponds to the boundary of the forbidden interval given by an ellipse; the ellipse elongates following the variation of t; limiting values of t correspond to an extremely elongated ellipse which degenerates into either a pair of parallel lines, Figure 10 or into a finite interval, Figure 11. In Figure 10 and Figure 11, the family of lines tends to the bound and the lines always belong to the permitted region. The forbidden region corresponds to the intersection of all ellipses that are the violation of a sufficient condition.

The envelope of the ellipses matches the forbidden region found by the necessary conditions, approximating it from outside. On the contrary, the necessary conditions approximate the same region from inside as a union of all forbidden regions corresponding to a given type of the variation.

Acknowledgements The authors gratefully acknowledge the anonymous referee whose suggestion helped to improve the exposition. This work was supported by NSF Grant No: DMS-0072717 and by ARO Grant No: 41363-MA.

References

Allaire, G. and Kohn, R. V. (1994). Optimal lower bounds on the elastic energy of a composite made from two non well-ordered isotropic materials. *Quarterly of Applied Mathematics*, LII(2):311–333.

Atkin, R. J. and Fox, N. (1980). *An Introduction to the Theory of Elasticity*. Longman Mathematical Texts, New York.

Bendsøe, M. P., Díaz, A. R., and Kikuchi, N. (1993). Topology and generalized layout optimization of elastic structures. In *Topology design of structures (Sesimbra, 1992)*, pages 159–205. Kluwer Academic Publishers Group, Dordrecht.

Bendsøe, M. P. (1995). *Optimization of Structural Topology, Shape, and Material*. Springer-Verlag, New York; Berlin; Heidelberg.

Cherkaev, A. V. (2000). *Variational Methods for Structural Optimization*, volume 140. Springer-Verlag, New York; Berlin; Heidelberg.

Cherkaev, A. V., Grabovsky, Y., Movchan, A. B., and Serkov, S. K. (1998a). The cavity of the optimal shape under shear stresses. *Int. J. Solids Struct.*, 35(33):4391–4410.

Cherkaev, A. V. and Kohn, R. V., editors (1997). *Topics in the mathematical modelling of composite materials*. Birkhäuser Boston Inc., Cambridge, MA.

Cherkaev, A. V., Krog, L. A., and Kucuk, I. (1998b). Staple optimal design of two-dimensional elastic structures. *Control and Cybernetics*, 27(2):265–282.

Cherkaev, A. V., Lurie, K. A., and Milton, G. W. (1992). Invariant properties of the stress in plane elasticity and equivalence classes of composites. *Proceedings of the Royal Society of London. Series A, Mathematical and Physical Sciences*, 438(1904):519–529.

Eschenauer, H. A. and Olhoff, N. (2001). Topology optimization of continuum structures: A review. *Appl Mech Rev*, 54(4):331–389.

Francfort, G. and Murat, F. (1986). Homogenization and optimal bounds in linear elasticity. *Arch. Rat. Mech. Anal.*, 94:307–334.

Fung, Y. C. (1965). *Foundation of Solid Mechanics*. Prentice-Hall, Upper Saddle River, NJ 07458.

Gibiansky, L. V. and Cherkaev, A. V. (1984). Design of composite plates of extremal rigidity. Report 914, Ioffe Physicotechnical Institute, Acad of Sc, USSR, Leningrad, USSR. English translation in Gibiansky and Cherkaev (1997).

Gibiansky, L. V. and Cherkaev, A. V. (1997). Design of composite plates of extremal rigidity. In Cherkaev, A. V. and Kohn, R. V., editors, *Topics in the Mathematical Modelling of Composite Materials*, volume 31 of *Progress in nonlinear differential equations and their applications*, pages 95–137. Birkhäuser Boston, Boston, MA. Translation. The original publication in Gibiansky and Cherkaev (1984).

Grabovsky, Y. (1996a). Bounds and extremal microstructures for two-component composites: A unified treatment based on the translation method. *Proceedings of the Royal Society of London. Series A, Mathematical and Physical Sciences*, 452(1947):945–952.

Grabovsky, Y. (1996b). Explicit solution of an optimal design problem with non-affine displacement boundary conditions. *Proceedings of the Royal Society of London. Series A, Mathematical and Physical Sciences*, 452:909–918.

Grabovsky, Y. and Kohn, R. V. (1995). Anisotropy of the Vigdergauz microstructure. *Journal of Applied Mechanics*, 62(4):1063–1065.

Hashin, Z. and Shtrikman, S. (1962). A variational approach to the theory of the elastic behavior of polycrystals. *J. Mech. Phys. Solids*, 10:343–352.

Küçük, I. (2001). *Variational approach to optimization of elastic structures*. PhD thesis, University of Utah.

Lurie, K. A. (1975). *Optimal Control in Problems of Mathematical Physics*. Nauka, Moscow, Russia. in Russian.

Lurie, K. A. and Cherkaev, A. V. (1978). Nonhomogeneous bar of extremal torsional rigidity. In *Nonlinear Problems in Structural Mechanics. Structural Optimization*, pages 64–68. Naukova Dumka, Kiev, Ukraine.

Milton, G. W. (1981). Bounds on the complex permittivity of a two-component composite material. *Journal of Applied Physics*, 52:5286–5293.

Milton, G. W. (1986). Modelling the properties of composites by laminates. In Ericksen, J. et al., editors, *Homogenization and Effective Moduli of Materials and Media (Minneapolis, Minn., 1984/1985)*, pages 150–175, New York; Berlin; Heidelberg. Springer-Verlag.

Milton, G. W. (2001). *The Theory of Composites*. 6. Cambridge Monographs on Applied and Computational Mathematics, Cambridge, UK. In Print.

Timoshenko, S. P. (1970). *Theory of Elasticity*. McGraw-Hill, New York.

Vigdergauz, S. B. (1989). Regular structures with extremal elastic properties. *MTT*, 24(3):57–63.